



**Oleogelating properties of ethylcellulose in oil-in-water emulsions
the impact of emulsification methods studied by ^{13}C MAS NMR, surface tension and
micropipette manipulation studies**

Munk, Merete B.; Utoft, Anders; Larsen, Flemming H.; Needham, David; Risbo, Jens

Published in:
Food Hydrocolloids

DOI:
[10.1016/j.foodhyd.2018.11.019](https://doi.org/10.1016/j.foodhyd.2018.11.019)

Publication date:
2019

Document version
Peer reviewed version

Document license:
[CC BY-NC-ND](https://creativecommons.org/licenses/by-nc-nd/4.0/)

Citation for published version (APA):
Munk, M. B., Utoft, A., Larsen, F. H., Needham, D., & Risbo, J. (2019). Oleogelating properties of ethylcellulose in oil-in-water emulsions: the impact of emulsification methods studied by ^{13}C MAS NMR, surface tension and micropipette manipulation studies. *Food Hydrocolloids*, 89, 700-706.
<https://doi.org/10.1016/j.foodhyd.2018.11.019>

Accepted Manuscript

Oleogelating properties of ethylcellulose in oil-in-water emulsions: The impact of emulsification methods studied by ^{13}C MAS NMR, surface tension and micropipette manipulation studies

Merete B. Munk, Anders Utoft, Flemming H. Larsen, David Needham, Jens Risbo

PII: S0268-005X(18)31633-3

DOI: <https://doi.org/10.1016/j.foodhyd.2018.11.019>

Reference: FOOHYD 4760

To appear in: *Food Hydrocolloids*

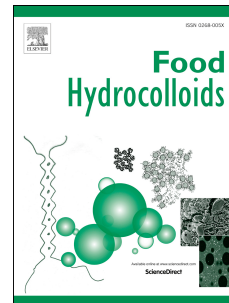
Received Date: 24 August 2018

Revised Date: 26 October 2018

Accepted Date: 7 November 2018

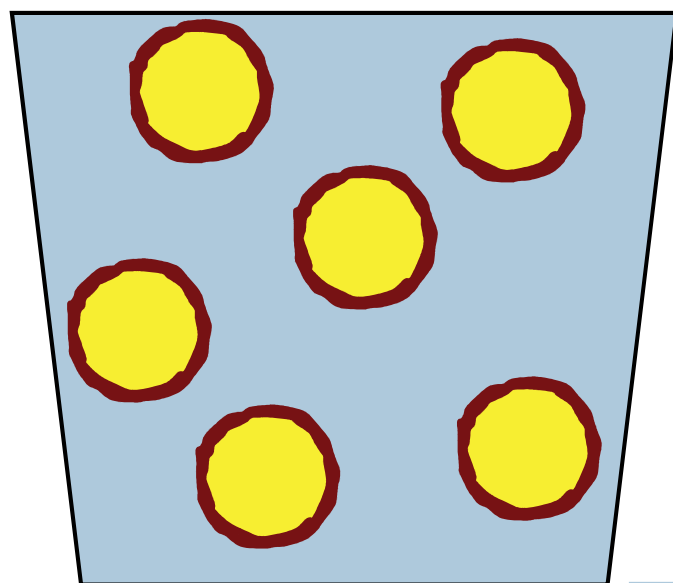
Please cite this article as: Munk, M.B., Utoft, A., Larsen, F.H., Needham, D., Risbo, J., Oleogelating properties of ethylcellulose in oil-in-water emulsions: The impact of emulsification methods studied by ^{13}C MAS NMR, surface tension and micropipette manipulation studies, *Food Hydrocolloids* (2018), doi: <https://doi.org/10.1016/j.foodhyd.2018.11.019>.

This is a PDF file of an unedited manuscript that has been accepted for publication. As a service to our customers we are providing this early version of the manuscript. The manuscript will undergo copyediting, typesetting, and review of the resulting proof before it is published in its final form. Please note that during the production process errors may be discovered which could affect the content, and all legal disclaimers that apply to the journal pertain.



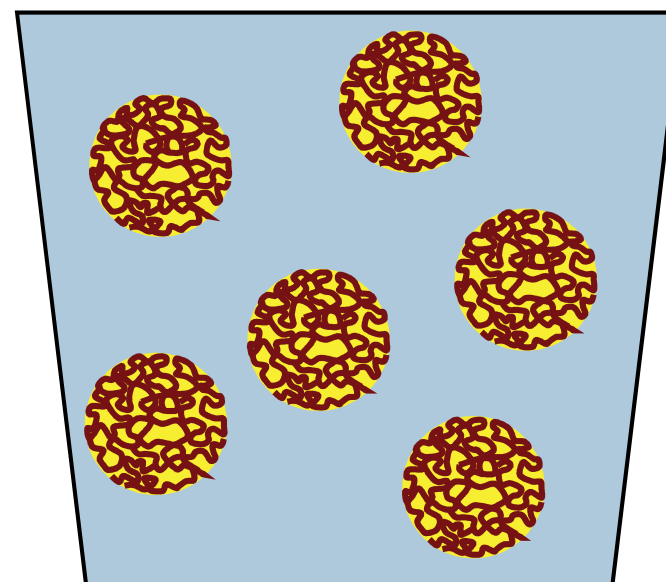
Hot emulsification

$$T > T_{\text{gel,EC}}$$



Cold emulsification

$$T < T_{\text{gel,EC}}$$



■ : H₂O

● : Oil

~ : EC

1 **Oleogelating properties of ethylcellulose in oil-in-water emulsions: The impact of emulsification methods**
2 **studied by ¹³C MAS NMR, surface tension and micropipette manipulation studies**

3 Merete B. Munk^{1*}, Anders Utoft², Flemming H. Larsen¹, David Needham^{2,3,4} and Jens Risbo¹.

4 ¹Department of Food Science, University of Copenhagen. Rolighedsvej 26, DK-1958, Denmark

5 ²Department of Molecular Medicine, University of Southern Denmark. Campusvej 55, 5230 Odense M,
6 Denmark

7 ³Department of Mechanical Engineering and Material Science, Duke University, Durham, NC 27708, USA

8 ⁴School of Pharmacy, University of Nottingham, Nottingham, UK

9 *Corresponding Author.

10 **Abstract**

11 This study addressed the oleogelating properties of EC when EC-oleogel microdroplets are dispersed in an
12 aqueous medium. By measuring the interfacial tension between oil-water, EC was found to be interfacial
13 active. Oleogel-in-water emulsions were prepared by two different emulsification methods termed *hot* and
14 *cold*. The first included high pressure homogenization of EC-oil and water at a temperature above the
15 gelling point of EC, whereas the latter implied dispersion of set EC-oleogels in water by high speed mixing at
16 a temperature below the melting point of EC-oleogels. The oleogelling functionality was lost when hot
17 emulsification was applied. Instead EC migrated to the interface of oil and water and formed a shell around
18 oil droplets which was assessed by micropipette manipulation techniques. On the other hand, the oleogel
19 remained stable when EC-oleogel was dispersed in water using the cold emulsification method. For this
20 system a fraction of the triglycerides in oil was immobilized in a similar manner as oil in bulk oleogels and
21 the mechanical properties of dispersed droplets were no longer reflecting the flow behavior of low viscous
22 oil, which indicates oil gelation by EC.

23 **Keywords:** Ethylcellulose, oleogel, emulsion, interfacial activity, solid-state NMR, micropipette
24 manipulation

25 **1. Introduction**

26 The desire to reduce the content of saturated fatty acids in the diet and the search for a more sustainable
27 replacement of palm oil has in recent years led to increased focus on ethylcellulose (EC) as an oleogelator.
28 EC is the only known food-grade polymer that can structure oil phases directly without applying costly

29 intermediate processing steps such as solvent exchange or solvent removal (Mattice & Marangoni, 2017).
30 Liquid oil can be gelled by heating the semi-crystalline EC in the oil above the glass transition temperature,
31 T_g , of EC and subsequently cool it below the gelling temperature, T_{gel} . T_g , T_{gel} , and the melting temperature,
32 T_m , of EC depend on its molecular weight, which is directly correlated with the polymer viscosity and
33 consequently EC is sold according to viscosity expressed in centipoise (cP) (Davidovich-Pinhas, Barbut, &
34 Marangoni, 2014, 2015a) . The physical properties of EC-oleogels are affected both by compositional and
35 processing parameters. Heating EC and oil above T_m (~180 °C) rather than T_g (~140 °C) results in oleogels of
36 higher mechanical strength as the polymer can reorganize itself when the entire fraction of crystals are
37 melted (Davidovich-Pinhas, Gravelle, Barbut, & Marangoni, 2015). High storage temperature of the molten
38 gel during setting is likewise increasing the strength of oleogels (Davidovich-Pinhas, Gravelle, et al., 2015).
39 Furthermore, a positive correlation between gel strength and enhanced polarity of the sample exists
40 regardless of the polar components that arise from oil oxidation, addition of surfactants or type of oil
41 (Davidovich-Pinhas, Barbut, & Marangoni, 2015b; Gravelle, Davidovich-Pinhas, Zetzl, Barbut, & Marangoni,
42 2016; Gravelle, Barbut, & Marangoni, 2012). The explanation for the gel strength being easily influenced by
43 such compositional changes is that EC-oleogels are based on inter-polymer junction zones created through
44 formation of hydrogen bonds between free unsubstituted hydroxyl groups (Laredo, Barbut, & Marangoni,
45 2011). At increased oil polarity additional hydrogen bonds between EC and oil are formed and
46 consequently the gel strength is enhanced (Gravelle et al., 2016).

47 By formation of oleogels it is hypothetically possible to mimic and thus replace saturated fat in food
48 products. In certain food products such as whipped cream, ice cream and baked goods the macromolecular
49 structure is highly dependent on crystallinity of saturated fatty acids though. In whipped cream and ice
50 cream elasticity opposing coalescence of dispersed fat globules allows formation of a three-dimensional
51 structuring network rather than coalescence of liquid droplets and furthermore elasticity of fat in pastries
52 provides a laminating effect between dough sheets and prevents cross-linking of gluten proteins
53 (Baardseth, Næs, & Vogt, 1995; Goff, 1997). This emphasizes the need for not only elucidating the physical
54 properties of bulk oleogels, but also to understand and optimize the behavior of oleogels in food product
55 matrixes if successful substitution of saturated fat should be implemented.

56 For the purpose of increasing the ratio of unsaturated fatty acids and decreasing the total fat content, EC
57 oleogels have been applied in laboratory scale to several food products such as cream cheese (Bemer,
58 Limbaugh, Cramer, Harper, & Maleky, 2016), comminuted meat products (Zetzl, Marangoni, & Barbut,
59 2012), and sausages (Barbut, Wood, & Marangoni, 2016). Overall, full or partial substitution by EC oleogels
60 was evaluated as promising ways to reduce the amount of saturated fat in these types of products.

61 Less focus has been directed toward EC-oleogel applications in emulsions such as whippable cream and ice
62 cream. Recently, EC was applied to ice cream produced with sunflower oil (Munk, Munk, Gustavson, &
63 Risbo, 2018), but the physical behavior of EC in this kind of emulsion system still needs to be clarified. As
64 the oleogel in such systems is dispersed as microdroplets, the gel formation and properties are not
65 straightforward to study as compared to bulk oleogels, and consequently other experimental techniques
66 besides rheology and texture analysis have to be employed. The objective of this study is to examine the
67 oleogelating properties of EC when EC-oleogels are dispersed in an aqueous phase. This was evaluated
68 according to two different emulsification procedures; one executed at temperatures above the gelling
69 point of EC (notated as hot method) whereas the other implied dispersion of the set oleogel at
70 temperatures below the gelling point of EC (notated as cold method). The studied emulsion matrix was
71 either based on an ice cream formulation or a simple oil-in-water model system depending on the analyses.
72 A combination of surface tension measurements, micropipette manipulation techniques and solid-state
73 NMR was combined to reach the objectives.

74 Utilization of EC to solidify liquid oil microdroplets of emulsions may open up for new possibilities to
75 interchange saturated fats with unsaturated oils in a wide range of food products. Most food either have a
76 high water activity or even a continuous aqueous phase in which the fat phase is dispersed. Therefore it is
77 of vital importance to investigate the physical behavior of EC in oil being in direct contact with an aqueous
78 phase.

79 **2. Materials & Methods**

80 Two grades of Ethylcellulose (EC), Ethocel Standard Premium 10 and 20, with viscosities of 10 and 20
81 centiPoise (cP) were provided by Dow Wolff Cellulosics, Bomlitz, Germany. Both grades of EC have a degree
82 of substitution around 2.5, whereas the chain length of the cellulose backbone differs and thus the
83 resulting viscosities. High oleic sunflower oil (HOSO), Fritex HOSO, was from AAK, Karlshamn, Sweden. A
84 distilled monoglyceride with high content of glycerol monooleate (GMO), Dimodan® MO 90/D, was used as
85 surfactant and provided by Dupont, Brabrand, Denmark. Guar gum, Grindsted Guar, and kappa
86 carrageenan, Carrageenan 100, used as stabilizers in emulsions were also from Dupont. Sodium caseinate,
87 Miprodan 30, and lactose were purchased from Arla, Brabrand, Denmark. Maltodextrin DE 15, C*Dry MD
88 01910, was from Cargill, Haubourdin, France, and sucrose from Nordic Sugar, Copenhagen, Denmark.

89 **2.1 Preparation of EC oleogels for NMR measurements**

90 Pure EC oleogels were prepared for NMR measurements. For the solid-state NMR analyses EC oleogels
91 were prepared by heating 10 wt% cP10 or cP20, 3 wt% GMO and 87 wt% HOSO to 180 °C under continuous

92 stirring on a hotplate magnetic stirrer and holding the mixture at this temperature for additionally 10
93 minutes to ensure complete melting of the polymer. The molten gel was immediately transferred to 4 mm
94 (o.d.) NMR rotors with a volume of 80 μ L using glass Pasteur pipette and cooled to ambient temperature.

95 **2.2 Preparation of EC oleogel-in-water emulsions**

96 EC oleogel-in-water emulsions were prepared for both NMR measurements and the micropipette
97 manipulation experiments. For the solid-state NMR analyses the composition of emulsions were tailored to
98 ice cream formulations: with 10 wt% HOSO, 1 wt% EC, and 0.3 wt% GMO in the lipid phase and 1 wt%
99 sodium caseinate, 12 wt% sucrose, 5 wt% lactose, 5 wt% maltodextrin, 0.15 wt% guar gum, and 0.02 wt%
100 carrageenan in the water phase. For micropipette droplet manipulation measurements the water phase
101 constituted just plain deionized water, as optical transparent samples are needed, **Figure 1**. Furthermore,
102 this technique requires larger droplets in order to study individual droplets, whereas solid-state NMR
103 analyses can be performed on realistic food emulsions containing small droplets sizes.

104 EC oleogel-in-water emulsions were prepared by two different methods referred to as *hot* and *cold*. For the
105 hot preparation, the water phase was heated to 80 °C in a water bath. Simultaneously, EC (cP10 and cP20),
106 GMO and HOSO were heated to 180 °C under continuous stirring, held at this temperature for 10 min, and
107 cooled to 90 °C whereupon it was mixed with the hot water phase. At this point, EC-oil was not set as a gel
108 but was still liquid. For the emulsions made for solid-state NMR analyses a heavy-duty laboratory mixer
109 (Silverson L4RT, Silverson Machines, Bucks, UK) was used for pre-homogenization followed by a two-stage
110 high-pressure homogenization at 150/50 bar (Panda Plus 2000, GEA Niro Soavi, Parma, Italy). A water bath
111 connected to the heating jacket of the feed hopper maintained the temperature of 80 °C during the entire
112 emulsification process. For the emulsions made for the micropipette droplet manipulation technique a
113 simple emulsification was performed by mixing the hot oil/EC and hot water on a vortex mixer for approx.
114 15 s.

115 The cold preparation method included formation of an EC-oleogel and a water phase. The EC-oleogel (cP10
116 and cP20) was produced by heating EC, HOSO and GMO to 180 °C for 10 min and subsequently cool it to
117 room temperature where it was allowed to set for approx. 24 h. The water phase was produced the
118 following day as described above for the hot methods, now with the modification that the water phase was
119 heated and subsequently cooled to room temperature before homogenization. In conclusion, cold
120 emulsified emulsions were homogenized at room temperature, **Figure 1**. For the emulsions made for solid-
121 state NMR analyses, homogenization was conducted with a high-speed blender (Omni-mixer homogenizer
122 17106, Sorvall, Newtown, CT, USA) equipped with 2 inch exterior rotor knives with an agitation speed of

123 16.000 rpm for 10 minutes. For the emulsions made for the micropipette droplet manipulation technique
 124 the emulsification was performed by mixing the oleogel and water phase approx. 15 s on a vortex mixer
 125 generating a wide range of droplet sizes. For the micropipette experiments, the emulsions were added to
 126 the microscope chamber so that droplets of appropriate sizes were chosen for micropipette manipulation.
 127 For NMR analyses, both emulsions from hot and cold preparation were transferred to 4 mm (o.d.) NMR
 128 rotors with a volume of 80 μ L using glass Pasteur pipette.

	Hot	Cold
NMR	Liquid-liquid homogenization High-pressure T = 80 °C Ice cream formulation (water phase: sugars, stabilizers, NaCas)	Gel-liquid homogenization High speed blender T = 20 °C Ice cream formulation (water phase: sugars, stabilizers, NaCas)
MDMT	Liquid-liquid homogenization Vortex mixer T = 80 °C Simple emulsion (deionized water)	Gel-liquid homogenization Vortex mixer T = 20 °C Simple emulsion (deionized water)

129

130 *Figure 1. Overview of homogenization methods of the emulsions prepared by the hot and the cold preparation for solid-*
 131 *state NMR and micropipette droplet manipulation technique (MDMT). For all emulsions, EC-oil had been undergoing*
 132 *thermal treatment at 180 °C, and then cooled to either 90 °C (still in liquid state: hot) or 20 °C (set gel: cold).*

133 2.3 Solid-state ^{13}C NMR spectroscopy

134 ^{13}C single-pulse (SP) magic angle spinning (MAS) and ^{13}C cross-polarization (CP) MAS NMR experiments
 135 were carried out at room temperature on a Bruker Avance 400 spectrometer (Bruker Biospin, Rheinstetten,
 136 Germany) operating at Larmor frequencies of 400.13 and 100.62 MHz for ^1H and ^{13}C , respectively, using a
 137 double-resonance probe equipped for 4 mm (o.d.) rotors. All spectra were recorded at a temperature of
 138 294 K and a spin-rate of 10000 Hz. For the SP/MAS experiments a recycle delay of 128 s and 300-512 scans
 139 were used, whereas a recycle delay of 8 s, 1024-6144 scans and a contact time of 1.0 ms (rf-field strength
 140 of 80 kHz for both ^1H and ^{13}C) were utilized for the variable amplitude CP/MAS experiments (Peersen, Wu,
 141 Kustanovich, & Smith, 1993). High-power TPPM (Bennett, Rienstra, Auger, Lakshmi, & Griffin, 1995) ^1H
 142 decoupling (rf-field strength: 80 kHz) was applied during an acquisition time of 49.2 ms. All spectra were
 143 referenced (externally) to the carbonyl resonance of α -glycine at 176.5 ppm.

144 Determination of the relative ratio of fatty acids and cellulose in the samples were obtained by integration
 145 of the spectral regions 11-22 ppm (A), 23-27 ppm (B) and 50-110 ppm (C). These regions represent the
 146 methyl groups from ethyl and the fatty acids, two specific carbons in the fatty acids (CH_2 next to methyl and
 147 $-\text{[CH}_2\text{]}-\text{CH}_2-\text{C=O}$), and cellulose + CH_2 from the ethyl, respectively. The molar fatty acid-to-cellulose ratio
 148 was then calculated as: $3 \cdot \text{int(B)} / (\text{int(C)} - \text{int(A)} + 0.5 \cdot \text{int(B)})$.

149 **2.4 Interfacial tension**

150 Solutions of EC (cP10 and cP20) in HOSO and sodium caseinate in MilliQ water respectively were prepared
151 in the following concentrations: 0.03%, 0.3%, 1.0% and 3.0%. EC was melted and dissolved in HOSO by
152 heating to 180 °C; solutions remained fluid as gelation is induced at concentrations >3%. The standard
153 micropipette method developed by Lee et al. (2001a, 2001b) was used for surface tension measurements
154 against air, where the micropipette was simply inserted into the microchamber, and was filled with air. For
155 the interfacial tension measurements between water and liquid oil solutions of EC, the oil phase was
156 loaded into the micropipette prior to insertion into the microchamber. The aqueous solution was kept
157 inside the microchamber and was aspirated under low controlled negative suction pressure into the
158 micropipette to form the interface of interest. Using calibrated-digital analysis, the standard way of
159 measuring interfacial tension is by placing a measuring box as seen in **Figure 2A**.

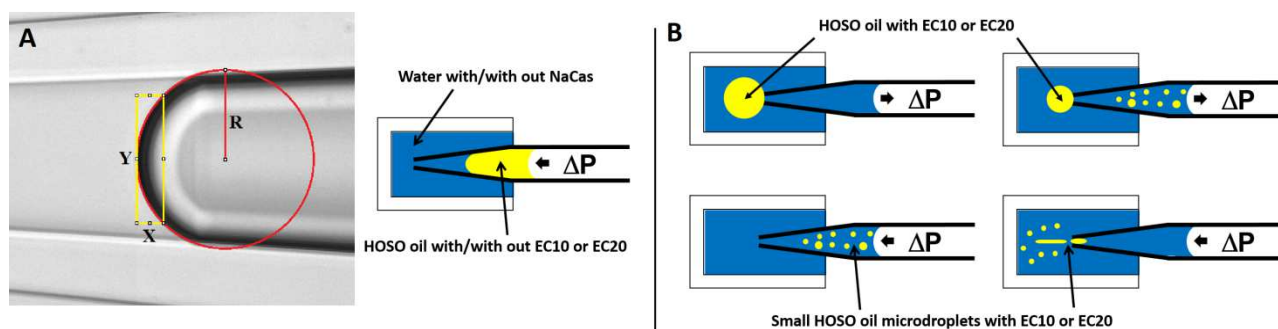
160 The box in **Figure 2A** gives a measure of X and Y, which are mathematically converted to the radius of
161 curvature, R_c , by using eq. 1.

$$R_c = \frac{\left(\frac{Y}{2}\right)^2 + X^2}{2X} \quad (1)$$

162 The radius of curvature can then be related to the interfacial tension using the Young–Laplace equation, eq.
163 2.

$$\Delta P = \frac{2\gamma}{R_c} \quad (2)$$

164 The pressure can then be changed several times, thus giving several pairs of pressure and radius of
165 curvature measurements. To obtain even more precise results than just calculating the interfacial tension
166 from a single measurement, a graph of ΔP vs $\frac{2}{R_c}$ can be constructed, resulting in the value of the slope
167 representing the interfacial tension in a much more precise fashion based on several measurements.



168

169 *Figure 2. A) Data acquisition from surface tension experiments. Example of the box (yellow) we use for extracting data*
 170 *for interfacial tension measurements. The box is placed so the left wall of the box just touches the meniscus, while the*
 171 *two right corners do the same. This takes place in the tapered part of the micropipette (interface between the blue and*
 172 *yellow phases), while making sure the oil phase extends into the parallel part of the micropipette. B) Micropipette*
 173 *manipulation of HOSO + EC emulsion in water. Larger microdroplets are located and caught with the micropipette.*
 174 *Increasing the suction pressure breaks the microdroplet into smaller microdroplets and sucks them into the micropipette.*
 175 *Reverting the suction pressure to blow the microdroplets back out deforms some of the microdroplets with diameters*
 176 *larger than the micropipette tip and microdroplet shape recovery or droplet-droplet interactions can be observed.*

177 **2.5 Micropipette droplet manipulation**

178 Coarse emulsions of EC oleogel-in-water were prepared as described above. Micropipettes with an o.d. of
 179 5-20 μm were prepared as described by Duncan et al. (2004, 2006) and used for the experiments. As seen
 180 in **Figure 2B**, microdroplets of the oil phase with an appropriate size range (10 - 50 μm) were selected for
 181 experiments. These larger microdroplets were located and caught with the micropipette using a low
 182 suction pressure. Increasing the suction pressure broke the microdroplet into smaller microdroplets and
 183 sucked them into the micropipette. Reversion of the suction pressure to blow the microdroplets back out of
 184 the micropipette tip provided information about mechanical properties of individual emulsified
 185 microdroplets, such as deformation and shape recovery.

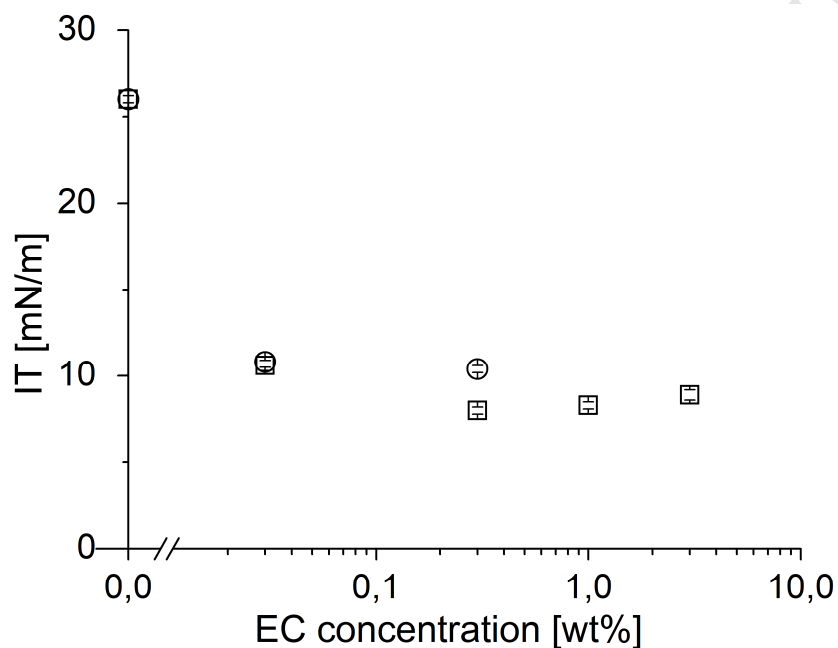
186 **3. Results**

187 **3.1 Interfacial activity of ethylcellulose**

188 The adsorption of surface active material at an interface between water and oil can be studied by
 189 measuring interfacial tension. That is, surface active components that accumulate in excess at the interface
 190 compared to bulk concentration will lower the interfacial tension. In order to deduce if EC accumulates at
 191 the oil/water interface, interfacial tension as function of EC concentration was measured as seen in **Figure**
 192 **3**. The interfacial tension of pure HOSO and water was 26 mN/m and adding as little as 0.03 % EC (the
 193 lowest measured concentration) reduced the interfacial tension to approx. 10 mN/m. Adding more EC cP10
 194 or EC cP20 had little effect as the data leveled off and, in any event, the measurements at high

195 concentration of EC were hindered by oil gelation. This behavior was also seen for other surface active
 196 polymeric systems like PEG (Gilányi, Varga, Gilányi, & Mészáros, 2006). The interfacial tension
 197 measurements show that EC is surface active and accumulates at the surface. For systems containing 0.3 %
 198 NaCas, a further reduction of the interfacial tension was measured with increasing concentration of EC,
 199 thus consolidating the surface active nature of EC even in presence of other surface active components
 200 (data not shown).

201



202

203 **Figure 3.** Interfacial tension of EC-HOSO solutions against pure water as a function of EC concentrations: EC cP10
 204 (square) and EC cP20 (circle).

205 3.2 Oleogels and hot emulsified oleogels

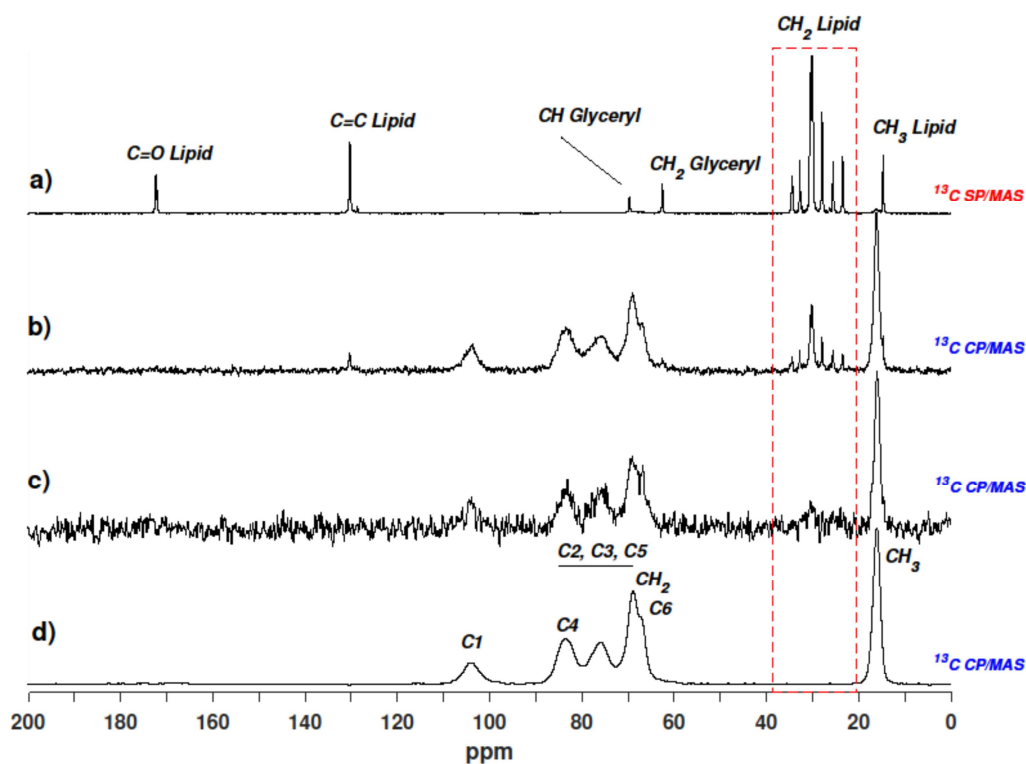
206 Next, we evaluated if and to what extent the oleogel could retain its gel properties when dispersed into an
 207 emulsion and put in contact with water. These experiments determined if and to what extent the physical
 208 characteristics of oleogels, especially their gelation properties, were changed as a consequence of
 209 emulsification and possibly uptake of water. These issues were addressed using ^{13}C -MAS NMR.

210 In this context, two NMR experiments were of particular importance. The carbon sites originating from the
 211 immobile regions of the sample were observed by ^{13}C CP/MAS NMR experiments, whereas all carbon sites
 212 were observed by ^{13}C SP/MAS NMR experiments. The reason for this selectivity is that polarization transfer
 213 from ^1H to ^{13}C by cross polarization (CP) requires non-vanishing hetero nuclear ^1H - ^{13}C dipolar couplings and
 214 those are only present in the immobile regions. In the mobile regions such dipolar couplings will be

215 averaged out due to fast liquid or liquid-like motion of the molecules. Due to the selectivity of the CP/MAS
216 data, only the SP/MAS data will provide a complete and quantitative description of the entire sample,
217 whereas the CP/MAS data enables characterization of the immobile part only. **Figure 4a)** shows the ^{13}C
218 SP/MAS spectrum of EC-oleogel containing 10 % EC cP20. As the oleogel contains nearly 90% HOSO and 10
219 % EC the ^{13}C SP/MAS spectrum shows that the oil constitutes the main part of the sample and the spectrum
220 is dominated by the carbons resonances from the triglycerides of HOSO. **Figure 4d** shows a ^{13}C CP/MAS
221 spectrum of the solid powder of EC and in this context it should be mentioned that CP/MAS and SP/MAS
222 spectra were identical as all carbons in this samples are immobile. In this spectrum the carbon sites of
223 glucose units as well as the ethoxy groups of EC were observed and assigned. Comparing **Figure 4a** and **4d**
224 it is seen that only low intensity peaks from EC is visible in the SP spectra of an oleogel and the most
225 obvious is the methyl resonance at 16.3 ppm.

226 The CP/MAS spectrum of the bulk oleogel (**Figure 4b**) is dominated by carbon sites from EC and thus this
227 component has a low mobility in oleogels. Besides the broad resonances from EC, a range of narrow
228 resonances with lower intensity originating from the lipids were present in the spectrum. Resonances from
229 unsaturated, methylene and methyl carbons in the lipids were observed, whereas no carbonyl from the
230 acid part of the fatty acids or carbons from the glycerol were detected. This indicates that the gelling
231 mechanism primarily involves the acyl tails of the triglycerides rather than the glycerol and ester bond
232 regions since the acyl tails are immobilized together with the EC. Comparison with the spectrum in figure 4a
233 demonstrates that although the oleogel appears firm and solid-like when handling and deforming the
234 material, only a minor fraction of the oil is immobilized in the EC oleogel. By integration the ratio of fatty
235 acids to glucose unit were determined to be approximately 7 to 100.

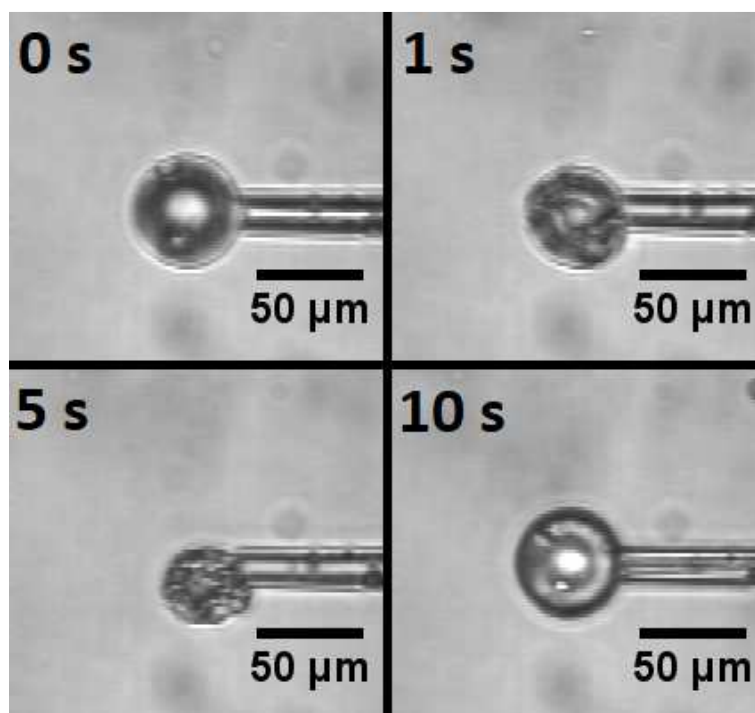
236 The corresponding ^{13}C CP/MAS spectrum of EC-oleogels dispersed in water by heating the oleogels and
237 applying high pressure homogenization at a temperature above T_{gel} shows NMR signals close to the noise
238 level for lipid CH_2 carbons and thus indicating no immobilization of acyl tails of triglycerides and loss of the
239 gelation effect of EC. No attempt was done to quantify the immobilized fatty acid chains as it was below the
240 limit of detection.



241

242 **Figure 4.** ^{13}C MAS NMR spectra of a) oleogel containing 10% EC cP20 applying single pulse SP/MAS, b) oleogel
 243 containing 10% EC cP20 applying cross polarization (CP)/MAS, c) CP/MAS spectra of 10% oleogel-in-water emulsion
 244 prepared using the hot emulsification method, d) CP/MAS spectra of pure EC cP20. The framed area shows the aliphatic
 245 hydrocarbons of triglyceride acyl chains. Identical NMR spectra were obtained for the analogous samples made with EC
 246 cP10.

247 Gelation of bulk oil and oleogelator has been clearly detected macroscopically as solidification of the
 248 material and it can be quantified in terms of gel hardness for example by texture analysis (Gravelle, Barbut,
 249 Quinton, & Marangoni, 2014). Such macroscopic techniques and evaluations are not an option for micron
 250 scaled dispersed droplets of oleogels in water. Instead evaluation of the properties of the dispersed oleogel
 251 emulsion was performed by micropipette droplet manipulation. This unique technique enables studies of a
 252 single microdroplet with a few microns of size while holding the microdroplet on the end of the
 253 micropipette by a low suction pressure. Microdroplets for this purpose were prepared by shaking molten
 254 EC oleogels and hot water. As shown by the times series of micrographs in **Figure 5**, a HOSO-EC
 255 microdroplet in water was gently aspirated from the suspension and held at the mouth of the micropipette.
 256 Upon the application of a low suction pressure, (at 1 s) the oil microdroplet started to move slowly into the
 257 micropipette. After 5 s the interior of the microdroplet was drained and only an exterior crumbled up shell
 258 remained. The microdroplet was restored by applying a small positive pressure thereby injecting the oil
 259 back into the shell (10 s).



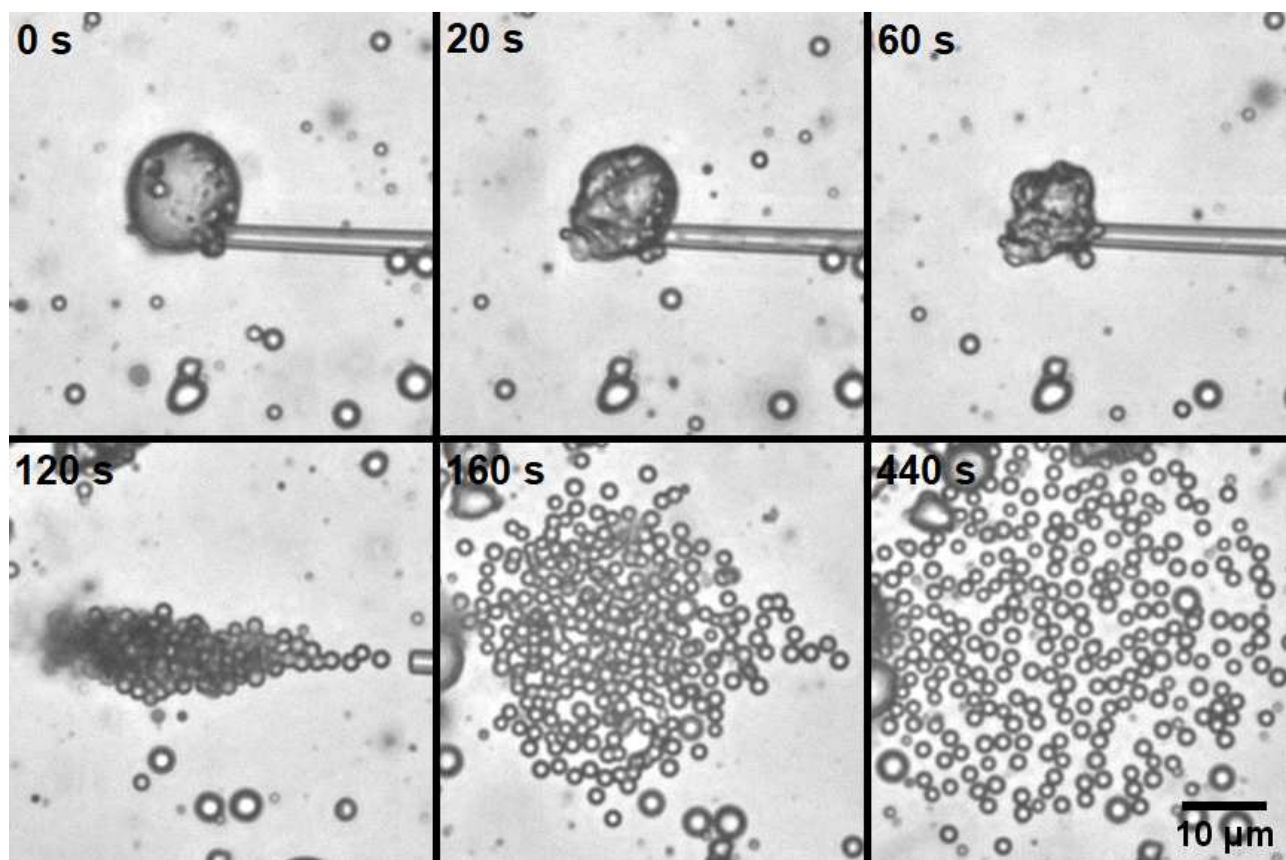
260

261 **Figure 5.** Video micrographs showing a HOSO-EC microdroplet in water, prepared by the hot emulsification method. At
 262 1 s the oil starts to be aspirated by the micropipette and after 5 s the oil is drained from the microdroplet and only an
 263 exterior crumbled up shell remains. The microdroplet can be restored by reverting the suction pressure and thereby
 264 injecting the oil back into the shell (10 s).

265 The fact that the internal oil can be separated from EC relatively easy and subsequently re-injected into the
 266 shell shows that the viscosity of the oil is rather low and consequently that some or all of the EC is most
 267 likely dispersed in the surrounding shell and thus not structuring the oil into a gel. This clearly showed that
 268 the interior of the oleogel was not a gel at all; it was simply a liquid oil microdroplet. Interestingly, the
 269 microdroplet had a fairly stable and relatively strong shell at its surface that remained intact during the
 270 draining of the interior and refilling. Hereby the micropipette study confirmed the observations by the ^{13}C
 271 MAS NMR data that oleogels are destroyed by hot emulsification.

272 3.3 Cold emulsified oleogels

273 It is a possibility that emulsification of the molten EC-oleogel in water enables the interfacially active EC to
 274 migrate to the interface of oil microdroplets and subsequently transform into solid-like surface material.
 275 From this viewpoint it was logical to attempt homogenization below T_{gel} at conditions where an EC-oleogel
 276 was formed and subsequently determine if access to water destroyed the gel.

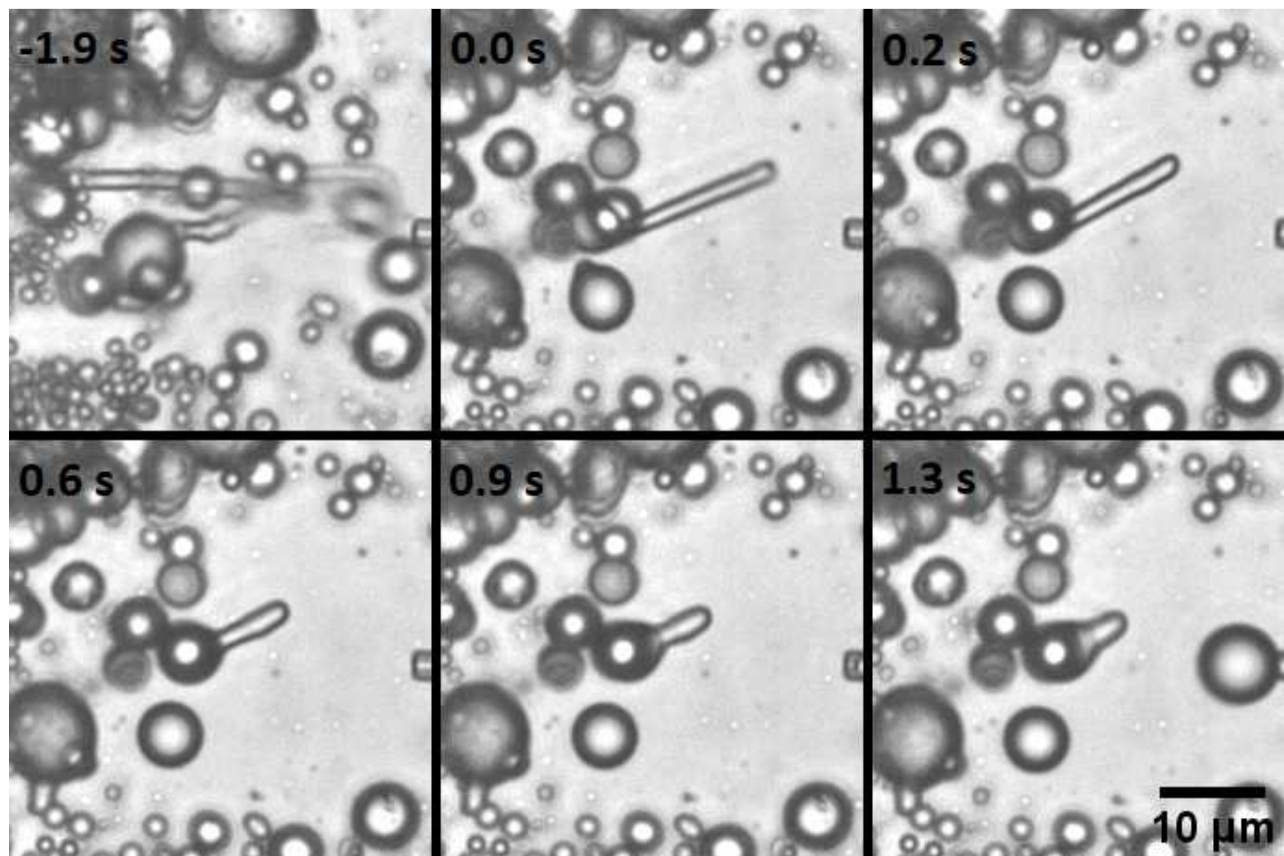


277

278 **Figure 6.** Video micrographs showing microdroplets of HOSO-EC dispersed in water by the cold emulsification method.
 279 The flowability of the oil is low, thus it takes longer time to aspirate the oil with the pipette (60 s). During reinjection of the
 280 oil, the exterior non-imbibed material is detached from the micropipette and instead many small oil droplets that remain
 281 stable and intact for prolonged periods are dispersed.

282 As shown in **Figure 6** one of the larger (15 μm diameter) cold-emulsified EC-oil droplets was gently
 283 aspirated and held at the tip of the micropipette. An increase in the suction pressure meant that material
 284 was again slowly aspirated into the micropipette, but this time the aspiration was considerably slower (60 s
 285 vs. 5 s for the hot emulsification method), indicating decreased flowability of the microdroplet interior.
 286 Unlike the exterior shell observed for the hot emulsified droplets, the non-imbibed material could not be
 287 refilled with oil, **Figure 6** (60 s). It merely detached from the pipette when attempting to reinject the oil. On
 288 the other hand, the material released from the pipette formed multiple smaller microdroplets that did not
 289 coalesce but remained stable despite close proximity and frequent collisions, **Figure 6** (160 s – 440 s).
 290 During material ejection into the chamber, tube-like morphologies were also observed which slowly within
 291 the time scale of one second slid back into the mother droplet, **Figure 7**. The slow time scale of the
 292 recovery of the shape indicates severe modification of the material compared to low viscosity oil. In
 293 comparison, in a previous study the recovery of droplets of a high viscosity liquid of 200 Pa s the time scale
 294 of recovery was in the order of 10 seconds (Tran-Son-Tay, Needham, Yeung, & Hochmuth, 1991). The

295 viscosity of pure HOSO is reported to be 0.067 Pa s (Quinchia, Delgado, Valencia, Franco, & Gallegos, 2009)
 296 and recovery of unstructured oil would be expected to happen within milliseconds and thus much faster
 297 than actually observed.

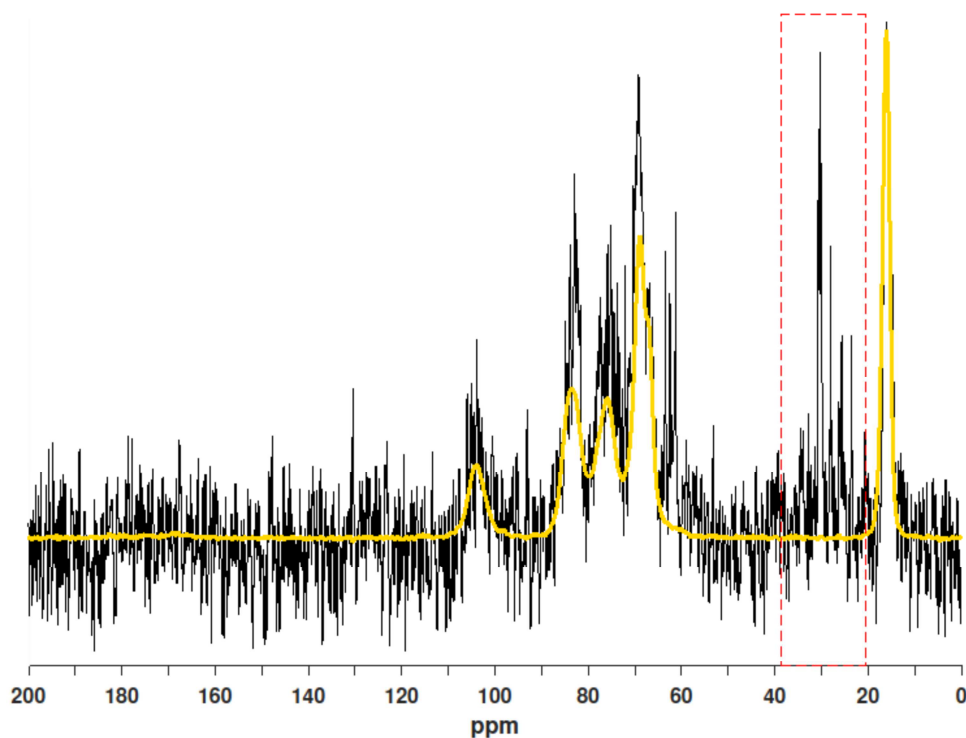


298

299 **Figure 7.** Video micrographs showing formation of a HOSO-EC microdroplet by injection of oleogel that has been
 300 subjected to cold emulsification method. A fraction of the injected oleogel forms a tube-like morphology that gradually
 301 merges with the mother droplet within the time scale of seconds.

302 The emulsions prepared by cold homogenization were studied using ^{13}C CP/MAS NMR as well. As for bulk
 303 EC-oleogels a small fraction of immobilized aliphatic carbon atoms of triglyceride acyl chains was observed,
 304 which indicates trapped triglycerides and thus formation of an oleogel as shown in **Figure 8**. By integration,
 305 the ratio of immobilized fatty acids to glucose units was determined to be about 8 per 100 glucose units
 306 and thus in the same order as bulk gels not in contact with water.

307 Identical ^{13}C CP/MAS NMR spectra for bulk EC-oleogels and oleogel emulsions combined with the slow
 308 recovery of oleogel microdroplets in micropipette experiments demonstrate that EC retains the ability to
 309 gel HOSO in emulsions if homogenization is performed at temperatures below the melting point of the
 310 oleogel.



311

312 **Figure 8.** ^{13}C CP/MAS NMR spectrum of 10% oleogel-in-water emulsion prepared using the cold emulsification method
313 (black). The NMR spectrum of EC is included as points of reference (yellow). The resonances of the immobilized
314 aliphatic methylene carbons from triglycerides are marked by the framed box.

315 4. Discussion

316 EC solubilized in oil is surface active and accumulates at the oil-water interface as seen by measurements of
317 interfacial tension. The micropipette manipulation technique revealed precipitation of EC into a solid state
318 present at the microdroplet interface. The solid state of EC is used for tablet coating in the pharmaceutical
319 industry and in contact with water (e.g. by ingestion) EC forms water insoluble films suitable for retarding
320 drug release in the gastro intestinal tract (Siepmann, Wahle, Leclercq, Carlin, & Siepmann, 2008). The effect
321 of water on EC in oil is in a way non-trivial as conventional oil-soluble components (such as oil soluble
322 vitamins) are not precipitated by dispersing the oil into water as an emulsion. The observed behavior of EC
323 could be explained by the following mechanism. At low temperature, the stable form of EC is in solid form
324 and the true solubility of this solid EC is low. Oil gelation using EC brings this component into a non-
325 equilibrium state. The contact with water of molten gels accelerates the conversion into the stable solid
326 form and particles of this stable form accumulate at the oil/water interface through a Pickering mechanism
327 (Dickinson, 2010). This suggests that the shell is not a single coherent entity but rather composed of
328 multiple EC particles. However, further studies are needed in order to determine the structure of the shell.

329 In the present study, it was observed that formation of an oleogel minced into fine pieces and dispersed in
330 water retained the oleogelating properties of EC. The mechanical properties of the interior of a
331 microdroplet no longer reflected the flow characteristics of low viscosity oil, which was supported by the
332 fact that a fraction of triglycerides was immobilized, as shown by ^{13}C MAS NMR studies. Actually, use of the
333 cold emulsification method has been the common way to incorporate EC-oleogels in food products such as
334 comminuted meat products and cream cheese (Barbut et al., 2016; Bemer et al., 2016; Zetzl et al., 2012),
335 even though the gelation properties of EC in relation to processing methods has not previously been
336 investigated.

337 The micropipette manipulation of cold emulsified EC oleogel microdroplets revealed slow recovery at a
338 timescale of seconds. Reinjection of a microdroplet formed tube-like morphologies that slide back into the
339 mother droplet rather than reverting to a compact more spherical shape. Such behavior can be related to
340 surface solidification and shape recovery dominated by a solid surface layer (Kim, Costello, Duncan, &
341 Needham, 2003). In this context, the micron scale structure of bulk EC oleogels must be discussed.
342 Structure of EC oleogels on this length scale has to our knowledge only been reported in one paper (Zetzl et
343 al., 2014). Here bulk oleogels are seen to contain oil pores of about 5 μm in diameter embedded in a rigid
344 and more solid EC/Oil matrix material. When such inhomogeneous material is dispersed into droplets with
345 diameters of 10-20 μm , it is likely that the matrix rich in EC will wet the surface and apolar oil pores will be
346 hidden in the interior of emulsion droplets. Such structure could explain the recovery behavior of tube
347 morphologies and the imbibing incapability of the exterior part of the droplet using a micropipette, but this
348 clearly needs to be confirmed by direct structural observations with an appropriate microscopic technique.

349 EC is added to the oil components in food products in order to obtain gelation of oil to mimic solid fats
350 containing large proportions of saturated triglycerides. The present study reveals that care should be taken
351 when assuming the same functionality of dispersed oleogels as in bulk oleogels and more special
352 techniques need to be employed to assess the state of EC in dispersed oil phases. Micropipette
353 manipulation can be used to observe droplets on micron scale in liquid emulsion systems and ^{13}C MAS NMR
354 is shown to be useful to monitor immobilization of parts of the fatty acid chains even in complex and solid
355 food matrices if other obscuring immobilized aliphatic carbon atoms are not present.

356 **5. Conclusion**

357 Mixing EC-oil mixtures with water at temperatures above the EC-oleogel set point will not result in an
358 oleogel, but form a shell or a film at the interface of the oil droplets. The lack of gel formation was
359 demonstrated by ^{13}C MAS NMR, and the presence of an interfacial shell by micropipette manipulation. In

360 contrast, if emulsions were prepared stepwise by initially making a set EC-oleogel and then disperse it into
361 water at temperatures below the melting point of the EC-oleogels, then EC would still work as an
362 oleogelator. This means that the oleogelating properties of EC can be utilized in O/W-emulsions when
363 applying the proper preparation method, and this opens up for potential use of EC as an oleogelating agent
364 in many emulsion-based food products.

365 **Acknowledgement**

366 This research was funded by Innovation Fund Denmark through the project “Ice cream with reduced
367 amount of saturated fat - a colloidal chemical approach”.

368 **References**

- 369 Barbut, S., Wood, J., & Marangoni, A. (2016). Quality effects of using organogels in breakfast sausage. *Meat*
370 *Science*, *122*, 84–89. <https://doi.org/10.1016/j.meatsci.2016.07.022>
- 371 Bemer, H. L., Limbaugh, M., Cramer, E. D., Harper, W. J., & Maleky, F. (2016). Vegetable organogels
372 incorporation in cream cheese products. *Food Research International*, *85*, 67–75.
373 <https://doi.org/10.1016/j.foodres.2016.04.016>
- 374 Bennett, A. E., Rienstra, C. M., Auger, M., Lakshmi, K. V., & Griffin, R. G. (1995). Heteronuclear decoupling in
375 rotating solids. *The Journal of Chemical Physics*, *103*(16), 6951–6958.
376 <https://doi.org/10.1063/1.470372>
- 377 Baardseth, P., Næs, T., & Vogt, G. (1995). Roll-in shortenings effects on danish pastries sensory properties
378 studied by principal component analysis. *LWT - Food Science and Technology*, *28*(1), 72-77.
379 [https://doi.org/10.1016/S0023-6438\(95\)80015-8](https://doi.org/10.1016/S0023-6438(95)80015-8)
- 380 Davidovich-Pinhas, M., Barbut, S., & Marangoni, A. G. (2014). Physical structure and thermal behavior of
381 ethylcellulose. *Cellulose*, *21*(5), 3243–3255. <https://doi.org/10.1007/s10570-014-0377-1>
- 382 Davidovich-Pinhas, M., Barbut, S., & Marangoni, A. G. (2015a). The gelation of oil using ethyl cellulose.
383 *Carbohydrate Polymers*, *117*, 869–878. <https://doi.org/10.1016/j.carbpol.2014.10.035>
- 384 Davidovich-Pinhas, M., Barbut, S., & Marangoni, A. G. (2015b). The role of surfactants on ethylcellulose
385 oleogel structure and mechanical properties. *Carbohydrate Polymers*, *127*, 355–362.
386 <https://doi.org/10.1016/j.carbpol.2015.03.085>
- 387 Davidovich-Pinhas, M., Gravelle, A. J., Barbut, S., & Marangoni, A. G. (2015). Temperature effects on the

- 388 gelation of ethylcellulose oleogels. *Food Hydrocolloids*, 46, 76–83.
389 <https://doi.org/10.1016/j.foodhyd.2014.12.030>
- 390 Dickinson, E. (2010). Food emulsions and foams: Stabilization by particles. *Current Opinion in Colloid and*
391 *Interface Science*, 15(1-2), 40-49. <https://doi.org/10.1016/j.cocis.2009.11.001>
- 392 Duncan, P. B., & Needham, D. (2004). Test of the Epstein-Plesset model for gas microparticle dissolution in
393 aqueous media: Effect of surface tension and gas undersaturation in solution. *Langmuir*, 20(7), 2567–
394 2578. <https://doi.org/10.1021/la034930i>
- 395 Duncan, P. B., & Needham, D. (2006). Microdroplet dissolution into a second-phase solvent using a
396 micropipet technique: Test of the epstein-plesset model for an aniline-water system. *Langmuir*, 22(9),
397 4190–4197. <https://doi.org/10.1021/la053314e>
- 398 Gilányi, T., Varga, I., Gilányi, M., & Mészáros, R. (2006). Adsorption of poly(ethylene oxide) at the air/water
399 interface: A dynamic and static surface tension study. *Journal of Colloid and Interface Science*, 301(2),
400 428–435. <https://doi.org/10.1016/j.jcis.2006.05.034>
- 401 Goff, H. D. (1997). Instability and Partial Coalescence in Whippable Dairy Emulsions. *Journal of Dairy*
402 *Science*, 80(10), 2620–2630. [https://doi.org/10.3168/jds.S0022-0302\(97\)76219-2](https://doi.org/10.3168/jds.S0022-0302(97)76219-2)
- 403 Gravelle, A. J., Barbut, S., & Marangoni, A. G. (2012). Ethylcellulose oleogels: Manufacturing considerations
404 and effects of oil oxidation. *Food Research International*, 48(2), 578–583.
405 <https://doi.org/10.1016/j.foodres.2012.05.020>
- 406 Gravelle, A. J., Barbut, S., Quinton, M., & Marangoni, A. G. (2014). Towards the development of a predictive
407 model of the formulation-dependent mechanical behaviour of edible oil-based ethylcellulose oleogels.
408 *Journal of Food Engineering*, 143, 114–122. <https://doi.org/10.1016/j.jfoodeng.2014.06.036>
- 409 Gravelle, A. J., Davidovich-Pinhas, M., Zetzel, A. K., Barbut, S., & Marangoni, A. G. (2016). Influence of solvent
410 quality on the mechanical strength of ethylcellulose oleogels. *Carbohydrate Polymers*, 135, 169–179.
411 <https://doi.org/10.1016/j.carbpol.2015.08.050>
- 412 Kim, D. H., Costello, M. J., Duncan, P. B., & Needham, D. (2003). Mechanical properties and microstructure
413 of polycrystalline phospholipid monolayer shells: Novel solid microparticles. *Langmuir*, 19(20), 8455–
414 8466. <https://doi.org/10.1021/la034779c>
- 415 Laredo, T., Barbut, S., & Marangoni, A. G. (2011). Molecular interactions of polymer oleogelation. *Soft*

- 416 *Matter*, 7(6), 2734-2743. <https://doi.org/10.1039/c0sm00885k>
- 417 Lee, S., Kim, D. H., & Needham, D. (2001a). Equilibrium and Dynamic Interfacial Tension Measurements at
418 Microscopic Interfaces Using a Micropipet Technique. 1. A New Method for Determination of
419 Interfacial Tension. *Langmuir*, 17(18), 5537–5543. <https://doi.org/10.1021/la0103259>
- 420 Lee, S., Kim, D. H., & Needham, D. (2001b). Equilibrium and dynamic interfacial tension measurements at
421 microscopic interfaces using a micropipet technique - 2. Dynamics of phospholipid monolayer
422 formation and equilibrium tensions at the water-air interface. *Langmuir*, 17(18), 5544–5550.
423 <https://doi.org/10.1021/la0103261>
- 424 Mattice, K. D., & Marangoni, A. G. (2017). Edible Applications of Ethylcellulose Oleogels. In A. R. Patel (Ed.),
425 *Edible Oil Structuring: Concepts, Methods, and Applications* (pp. 250–274). The Royal Society of
426 Chemistry. <https://doi.org/10.1039/9781788010184-00250>
- 427 Munk, M. B., Munk, D. M. E., Gustavson, F., & Risbo, J. (2018). Using Ethylcellulose to Structure Oil Droplets
428 in Ice Cream Made With High Oleic Sunflower Oil. *Journal of Food Science*, 83(10), 2520-2526.
429 <https://doi.org/10.1111/1750-3841.14296>
- 430 Peersen, O. B., Wu, X., Kustanovich, I., & Smith, S. O. (1993). Variable-amplitude cross-polarization MAS
431 NMR. *Journal of Magnetic Resonance - Series A*, 104(3), 334–339.
432 <https://doi.org/10.1006/jmra.1993.1231>
- 433 Quinchia, L. A., Delgado, M. A., Valencia, C., Franco, J. M., & Gallegos, C. (2009). Viscosity modification of
434 high-oleic sunflower oil with polymeric additives for the design of new biolubricant formulations.
435 *Environmental Science and Technology*, 43(6), 2060–2065. <https://doi.org/10.1021/es803047m>
- 436 Siepmann, F., Wahle, C., Leclercq, B., Carlin, B., & Siepmann, J. (2008). pH-sensitive film coatings: Towards a
437 better understanding and facilitated optimization. *European Journal of Pharmaceutics and*
438 *Biopharmaceutics*, 68(1), 2–10. <https://doi.org/10.1016/j.ejpb.2007.03.025>
- 439 Tran-Son-Tay, R., Needham, D., Yeung, A., & Hochmuth, R. M. (1991). Time-dependent recovery of passive
440 neutrophils after large deformation. *Biophysical Journal*, 60(4), 856–866.
441 [https://doi.org/10.1016/S0006-3495\(91\)82119-1](https://doi.org/10.1016/S0006-3495(91)82119-1)
- 442 Zetzi, A. K., Gravelle, A. J., Kurylowicz, M., Dutcher, J., Barbut, S., & Marangoni, A. G. (2014). Microstructure
443 of ethylcellulose oleogels and its relationship to mechanical properties. *Food Structure*, 2(1–2), 27–40.
444 <https://doi.org/10.1016/j.foostr.2014.07.002>

445 Zetzl, A. K., Marangoni, A. G., & Barbut, S. (2012). Mechanical properties of ethylcellulose oleogels and their
446 potential for saturated fat reduction in frankfurters. *Food & Function*, 3(3), 327–337.
447 <https://doi.org/10.1039/c2fo10202a>

448

ACCEPTED MANUSCRIPT

Highlights:

- Homogenization temperature is crucial for gelling properties of EC in O/W-emulsions
- EC forms a shell around oil droplets when emulsified at high temperatures
- EC-oleogel droplets remain gels when emulsified below melting temp of EC-oleogels
- ^{13}C MAS NMR is an excellent technique to study oleogels in complex food systems